

# The Burning Velocity of Pulverised Biomass: the Influence of Particle Size

Muhammad Azam Saeed, David M. Slatter, Gordon E. Andrews\*, Herodotos N. Phylaktou, Bernard M. Gibbs

School of Chemical and Process Engineering, University of Leeds, Leeds, LS2 9JT, UK  
[profgeandrews@hotmail.com](mailto:profgeandrews@hotmail.com)

The use of pulverised biomass as a replacement for coal in power generation is a major source of renewable electricity in the UK. However, there is little data on flame propagation rates for pulverised biomass and this makes it difficult to design burners and model these flames using the traditional burning velocity approach. An ISO 1 m<sup>3</sup> dust explosion vessel was modified to enable constant pressure spherical expanding turbulent flame speeds,  $S_T$ , to be measured for pulverised biomass. The turbulence generated by the new dust injection system was calibrated using turbulent and laminar gas explosions and this enabled the dust laminar flame speed,  $S_L$ , to be determined from  $S_T$ . The burnt gas expansion ratio,  $E_P$ , was determined from the peak pressure rise and this enabled the laminar burning velocity,  $S_u$ , to be determined from the measured  $S_T$ . The results showed for a range of biomass that the peak  $S_T$  was in the range 3–5.5 m/s. The laminar burning velocity for 26 biomass and two coal samples and were very low at 0.1 – 0.2 m/s for the most reactive mixture, depending on the biomass particle size.

## 1. Introduction

Pulverised biomass for electric power generation in coal fired power plants accounted for 5.7% of all electricity generated in the UK in 2014. Modelling of gas and dust burner flames and explosions requires knowledge of the laminar burning velocity,  $S_u$ . For dust flames there is no agreed methodology for the measurement of  $S_u$  and hence no agreed values that can be used in explosion protection design or in pulverised biomass burner design. Andrews and Bradley [1972] showed that there were systematic errors in most methods of determining the laminar burning velocity of gases and these were related to the finite thickness of the flame and the assumption of an infinitely thin flame in many of the measurement methods. As the flame thickness of dust flames is greater than gas flames, the measurement problems of  $S_u$  for dusts are greater than for gas flames. Some recommended values of  $S_u$  for gases, using measurement methods with low errors, were recommended by Andrews and Bradley [1972] and adopted in NFPA68 [2013]. For dusts no data base exists for  $S_u$ , as reliable measurement methods don't exist. The lack of a standard for the measurement of  $S_u$  for gases or dusts contrasts with dust flammability limits, where standards do exist [EN1839:2013].

In gas or dust explosion protection design using venting or suppression there has always been a requirement to take into account the reactivity of the most reactive mixture. The deflagration parameter,  $K$ , has been used for the mixture reactivity in explosion venting guidance [NFPA, 2013]. This is determined in a closed spherical vessel explosion by measuring the maximum rate of pressure rise ( $dP/dt_{max}$ ) [EN15967:2011; EN14036-2:2006] times the cube root of the volume,  $V$ ,  $K = (dP/dt_{max}V^{1/3})$  bar m/s. For gases this is referred to as  $KG$  and for dusts  $K_{st}$ . Also required to is the peak explosion pressure,  $P_{red}$ , and there are standards on how to do this [EN14034:2007]. These reactivity parameters are embedded in the European standards for gas [EN14994:2007] and dust venting [EN14491:2012], but are not used in combustion modelling.

The measurement procedures for the dust reactivity,  $K_{st}$ , require the ISO standard [ISO 6184/1] 1m<sup>3</sup> spherical explosion vessel to be used to determine  $P_{msx}$  and  $dp/dt_{max}$ . The standard dust explosion techniques are based on a turbulent dust injection process, as turbulence is required to keep the dust dispersed. The average turbulence can be calibrated by undertaking laminar gas explosions and then operating the air injection system into a premixed gas air mixture to generate the same turbulence as occurs in the dust explosion

[Gardner et al., 2001; Satter et al., 2014; Bartknecht, 1989]. Up to 2012 the KG reactivity parameter for gases [Bartknecht, 1993] was part of the gas venting design standards in the USA [NFPA68, 2007] but have been replaced by a more fundamental gas venting design procedure based on  $S_u$  [NFPA68, 2013]. However, they have not regulated how  $S_u$  is measured but have specified a reference value for propane of 0.46 m/s. They also continue to use  $K_{st}$  as the reactivity parameter for dust. The problem with the KG approach to gas reactivity is that it is dependent on the vessel volume [NFPA68, 2007], due to self-acceleration of the flame caused by the formation of cellular flames. The procedures of Chippett [1984] are used in the USA gas venting standards [NFPA68, 2013] to increase  $S_u$  due to this effect, but there is no similar procedure in the European venting standards [EN14491:2012].

Andrews and Phylaktou [2010] showed that for gases the  $K_G/P_i$  and  $S_u$  gas reactivity parameters are linearly related by Eq. 1.

$$K_G/P_i = 3.16 (P_m/P_i - 1) S_u E_p \quad \text{m/s} \quad (1)$$

They also showed that for reasonable values of  $S_u$  and adiabatic  $P_m/P_i$  the predicted values of  $K_G$  were in reasonable agreement with experimental  $K_G$  measurements. For dusts Cashdollar [2000] proposed that  $E_p$  could be determined as the ratio of peak pressure to initial pressure in a closed vessel dust explosion, as it is quite difficult to calculate for dusts, and this was used in the present work. Sattar et al. [2014] showed for the first time that  $K_G$  and  $S_u$  were linearly related as in Eq. 1, but only if both reactivity parameters were measured in the same explosion vessel. They showed that the ISO 1 m<sup>3</sup> vessel was the ideal vessel size to measure  $S_u$  for gases by measuring the laminar flame speed,  $S_L$ , and was the minimum size that made the common assumption of an infinitely thin flame and the consequent relationship in Eq 2 to be valid.

$$S_u = S_L/E_p \quad (2)$$

Sattar et al. [2014] used this approach to determine the maximum  $S_u$  of methane-air to be 0.42 m/s which they showed to be in good agreement with a wide range of other measurements using reliable techniques [Andrews and Bradley, 1972]. This approach was applied to a range of pulverised biomass in the present work using measured  $S_T$  for dust/air mixtures and a calibrated turbulence factor of 4.7.

## 2. Laminar Burning Velocity of Dusts

The most common method of burning velocity measurements for dusts is to use the vertical tube method with dust falling from the top and ignition at the bottom [Proust, 1993]. Andrews and Bradley [1972] showed that this method did not give reliable values of  $S_u$  for gas/air mixtures and the same is likely for dust/air explosions. Proust and Veyssiere [1988] used this method for maize starch and measured a maximum  $S_u$  of 0.3 m/s; Wolanski [1995] reported a value of 0.55 m/s for maize starch using a similar technique. Mazarkiewicz and Jorisade [1994] measured the maximum  $S_u$  of cornstarch at 0.14 m/s. Nagy and Veritas [1983] developed a method to use the Hartmann vertical tube dust explosion equipment to measure the maximum  $S_u$  for a wide range of materials with maximum  $S_u$  0.02 – 0.1 m/s, which are similar to those in the present work. Dahoe et al. [2002] reported the maximum  $S_u$  of cornflour as 0.63 m/s and Smoot et al. [1977] determined the maximum  $S_u$  of lignite as 0.31 m/s for 10  $\mu\text{m}$  particles and 0.21 m/s for 33  $\mu\text{m}$  particles.

Phylaktou et al. [2011] measured  $S_u$  from Eq. 2 for several dusts for the maximum reactivity mixtures, using the present ISO 1 m<sup>3</sup> spherical vessel. They increased the ignition delay between the start of dust injection and the firing of the ignitor, so as to allow the initial turbulence to decay to zero.  $S_u$  for maize starch was determined as 0.25 m/s. For biscuit flour  $S_u$  was 0.20 m/s, for a coal it was 0.17 m/s, for milk powder it was 0.14 m/s and for resin powder, which is mainly a hydrocarbon dust, it was 0.48 m/s which is typical of high MW hydrocarbon gas burning velocities. However, this method has the weakness of the result being an extrapolation of the curve fit of  $S_T$  as a function of the ignition delay to infinite delay and although the above  $S_u$  data are reasonable, the accuracy is uncertain.

Sattar et al. [2014] developed an alternative method for using the ISO 1 m<sup>3</sup> dust explosion equipment for  $S_u$  measurement, which is used in the present work. The ratio of the turbulent to laminar flame speeds for gases in the ISO 1m<sup>3</sup> dust explosions was determined as 4.0, for the standard 'C' ring and ignition delay and this was applied to the measured turbulent dust/air flame speeds,  $S_T$ , to determine the laminar flame speed,  $S_L$ . Then  $S_u$  was calculated using Eq. 2 with the expansion ratio determined from the measured peak to initial pressure ratio [Cashdollar, 2000]. Sattar et al. [2014] measured the maximum  $S_u$  of cornflour as 0.55 m/s, walnut shell dust as 0.55 m/s and Kellingley coal as 0.17 m/s.

### 3. Experimental Equipment

The dust explosion vessel was manufactured to the ISO specification [ISO 618511], where the vessel is more like a cylinder with rounded edges and the volume is  $1.138 \text{ m}^3$ . This was calibrated for the ratio of turbulent to laminar gas explosions as 4.0 [Satter et al. 2011]. This value is also supported by Bartknecht [1989, 1993] using the  $K_G$  ratio. The ignition source for dusts was a 10 kJ chemical ignitor [ISO 618411]. Two 5kJ chemical ignitors were directed against a small hemispherical cap to produce a spherical ball of hot gases that resulted in spherical flame propagation. For both gas and dust explosions the flame speed was determined by the time of arrival of flames at an array of exposed junction Type K mineral insulated thermocouples. These were located in two planes at  $90^\circ$  to each other so that spherical flame propagation could be demonstrated. Sattar et al. [2014] showed for flame diameters up to 800mm the pressure rise was  $<1\%$ , so that constant pressure burning velocities were measured. When the flame was close to the spark at flame diameters,  $<200\text{mm}$ , the flame speed was influenced by the flame curvature [Satter et al., 2012, 2014] and for dust explosions it was influenced by the initial ball of hot chemical ignitor products. Beyond flame diameters of 800mm the rise in pressure and temperature due to compression would influence the flame speed. For gases flame instabilities lead to cellular flames that cause flame acceleration if the flame diameter is large enough. The approach of Chippett [1984], adopted in NFPA68 [2013], predicts that for flame diameters up to 800mm the flame self-acceleration will be  $<10\%$ . For these reasons the flame speed was determined between 200 and 800mm diameter or a 300mm flame travel distance. This flame was sufficiently large in diameter for the assumption of an infinitely thin flame front and Eq. 2 to be valid. Sattar et al. [2014] showed that these measurement procedures gave a maximum  $S_u$  for methane-air of 0.42 m/s, which was comparable with literature measurements for accurate methods [Andrews and Bradley, 1972].

Using pulverized fibrous biomass in the ISO  $1 \text{ m}^3$  explosion vessel has several problems. The bulk density of the biomass means that the 5L external pot is not big enough to hold sufficient mass for the maximum flame reactivity concentration. This problem was solved by Sattar et al. [2013] using a 10L external volume to hold the biomass pressurized to 10 bar, so that the same external air mass was used. Fibrous biomass will not pass through the standard 'C' ring disperser and this led to a development programme of alternative injection systems. The rebound nozzle [ISO618411, Bartknecht, 1993] would also not pass fibrous biomass dust. For many dusts sieved  $<63\mu\text{m}$  it was found that an injection system similar to that used for dry powder explosion suppression systems was viable and gave spherical flames. This is a spherical grid plate with holes over the hemisphere facing away from the wall. Huescar-Medina et al. [2013] calibrated this according to the above procedures with a turbulence factor of 4.0 for the standard C ring with the standard 0.6s delay time. This was used in the present work for some of the fibrous biomass sieved to  $<63 \mu\text{m}$ .

For many fibrous biomass, that are difficult to mill, even sieving to  $<63\mu\text{m}$  did not result in a powder that would flow from the external pot to the spherical injector. The method shown in the ISO618411 dust explosion standard was developed. The dust was placed at the bottom of the vessel in a hemispherical container with compressed air from the external pot directed through a pipe into the biomass dust. It was found that this only gave a spherical flame if dispersion holes at the end of the pipe were used with the same area and number as in the standard C ring injector. This was calibrated using gas explosions and compared with cornstarch explosions, where a 0.5s delay was required for the same  $K_{st}$  and the turbulence factor was 4.7, close to that of 4.0 for the standard 'C' ring, the presence of dust increases the turbulence.

### 4. Biomass and Comparative Dust Compositions

Table 1 lists the properties of all the biomass investigated. The stoichiometric A/F was computed on a dry ash free basis (daf) and on an actual basis [Andrews and Phylaktou, 2010]. These values are used to determine the equivalence ratios of the burnt biomass concentration. The biomass dusts were all sieved to  $<63\mu\text{m}$ , but size analysis of the pulverised powders using laser light scatter, showed a very wide size distribution that was different for each biomass. SEM analysis of the particles showed that the fibrous biomass were cylindrical in the shape of the particles but longer than  $63\mu\text{m}$ , with a diameter  $<63\mu\text{m}$  that slipped vertically through the sieve. For nut shell biomass such as walnut, which undergoes brittle fracture, the particles were more cubic and similar to pulverised coal. These particles will pass through the standard C ring [Satter, 2013]. Also listed in Table 1 are thermally processed biomass materials, torrefied [Satter et al., 2012] or steam exploded [Saeed et al., 2016]. These processes lose some of the volatiles, but the main effect is to reduce the particle size as the torrefied particles are brittle. Some non-biomass dusts have been included, which have been investigated using the same equipment. Table 1 shows that on a daf basis the volatile content of the biomass particles was very high and had a relatively small range of 73.5 – 92.3%, which is similar to the four reference standard dusts of similar HCO composition milk powder, biscuit flour, cornflour and lycopodium, which are not fibrous materials and have a volatile range 88 – 94.6%.

## 5. Results

A feature of dust explosions in the ISO 1 m<sup>3</sup> equipment, that is rarely commented in the literature, is that about half of the powder injected remains on the floor of the vessel at the end of the test [Satter et al., 2012]. This means that the concentration of the dust in the flame that propagated is not that given by the injected concentration. The mass of dust at the end of the test was vacuumed out of the vessel and weighed. Chemical analysis of the debris showed that it was predominantly the original biomass with the same size distribution.

Table 1 Chemical Characterisation of biomass in comparison to two coal samples

Biomass	Labels	Ultimate analysis					Proximate analysis					Bomb cal.	Stoich. calc.	
		C (%)	H (%)	O (%)	N (%)	S (%)	H <sub>2</sub> O (%)	VM (%)	VM (%)	FC (%)	Ash (%)	CV (MJ/Kg)	Stoich. A/F	Stoich. A/F Actual
		daf	daf	daf	daf	daf	ar.	ar.	daf	ar.	ar.	actual daf	daf.	(g/g)
Bagasse	B	55.6	7.3	35.7	1.3	0.1	7.2	67.1	92.3	5.6	20.1	15.6 21.5	7.5	5.4
Rice Husk	RH	49.8	6.4	42.7	1.1	0.0	7.7	62.3	83.7	12.2	17.9	15.2 20.4	6.2	4.6
Wheat Straw	WS	50.6	6.4	41.5	1.4	0.1	6.8	60.7	86.2	9.7	22.8	14.5 20.6	6.4	4.5
Corn Cobs	CC	45.9	6.0	46.8	1.2	0.1	7.1	69.4	82.5	14.8	8.8	14.8 17.6	5.4	4.5
Peanut Shell	PS	53.7	6.6	38.2	1.5	0.0	7.00	66.4	78.1	18.6	8.0	18.2 21.4	6.9	5.9
Steam exploded wood	BP	52.8	5.8	41.0	0.4	0.0	4.4	73	78.6	19.9	2.7	19.5 21.0	6.28	5.8
Walnut shell	WAL	52.9	6.8	39.6	0.6	0.1	5.0	74.6	84.0	14.2	6.3	19.2 21.7	6.8	6.0
Pistachio nut shell	PIS	49.4	6.3	41.7	2.6	0.0	2.7	78.4	88.1	10.7	8.3	18.2 20.4	6.2	5.5
Corn flour	CF	44.7	7.4	47.8	0.1	0.0	11.6	77.8	92.0	6.8	3.8	16.4 19.4	5.7	4.8
Lycopodium	LC	68.2	9.4	20.4	2.0	0.0	1.6	89.2	94.6	5.1	4.1	29.6 31.4	10.4	9.8
Oak sawdust	OAK	51.4	6.5	41.8	0.2	0.0	8.9	72.7	84.6	13.3	5.1	20.0 23.3	6.4	5.5
Pine wood mixture	PWP	49.7	7.0	42.6	0.7	0.0	3.5	79.5	90.0	8.7	8.2	19.2 21.7	6.3	5.6
Milk powder	MP	52.4	7.7	35.2	4.4	0.2	4.6	79.2	88.0	10.7	5.4	22.3 24.8	7.5	6.8
Biscuit flour	BIS	40.7	5.6	51.0	2.7	0.0	11	78.4	92.1	6.8	3.9	14.8 17.4	4.5	3.9
SPF wood mixture	SPFR	50.5	7.0	41.4	1.2	0.0	7.8	73.5	82.0	16.2	2.6	18.3 20.4	6.4	5.7
SPF torrefied	SPFT	54.7	6.9	37.4	1.1	0.0	4.0	74.6	80.4	18.2	3.2	20.8 22.4	7.1	6.6
Whole tree wood (Raw and torrefied)	ECNR	52.9	6.3	40.9	0.0	0.0	5.3	78.0	85.9	12.8	3.9	18.9 20.8	6.5	5.9
	ECNT	52.7	6.2	40.8	0.3	0.0	2.0	78.2	82.6	16.5	3.3	20.1 21.2	6.5	6.2
Wood (Raw and torrefied)	RWER	47.0	6.1	44.7	2.2	0.0	4.6	83.4	92.4	6.8	5.1	18.3 20.3	5.8	5.2
	RWET	56.0	6.0	35.2	2.7	0.0	3.9	68.9	78.6	18.8	8.4	20 22.8	7.3	6.4
Norway spruce (Raw and torrefied samples at different conditions)	S2SR	53.4	6.2	40.3	0.0	0.0	5.8	79.0	87.7	11.1	4.1	19.2 21.3	6.5	5.9
	S2STS	55.5	5.6	38.1	0.8	0.0	2.8	77.0	82.8	15.9	4.2	21.8 23.4	6.7	6.2
	S2STA	59.9	5.7	33.6	0.8	0.0	2.7	69.4	75.8	22.1	5.8	20.8 22.5	7.5	6.9
	S2STB	58.6	5.3	35.3	0.7	0.0	3.4	63.6	73.6	22.8	10.2	20.0 23.1	7.1	6.1
Southern pine (Raw and torrefied)	NBER	52.3	5.8	41.2	0.6	0.0	5.0	78.5	84.9	14.0	2.5	19.4 21	6.3	5.8
	NBET	58.4	5.6	35.2	0.8	0.0	3.3	70.3	76.1	22.1	4.3	21.6 23.4	7.2	6.7
Kellingley Coal	K Coal	82.1	5.2	7.0	3.0	0.1	1.7	29.2	36.9	50	19.1	25.0 31.6	11.6	9.2
Colombian Coal	C Coal	81.7	5.3	9.6	2.6	0.0	3.2	33.7	41.3	47.8	15.3	26.4 32.4	11.2	9.1

The mass burnt in the explosion was determined as the mass injected minus any mass that remained in the injection pot, minus the mass collected on the vacuum bag. This burnt dust concentration after correcting for burnt mass ash was expressed as a burnt dust equivalence ratio, using the dust stoichiometric A/F in Table 1. An explosion induces a wind ahead of the expanding flame and this interacts with the particles through particle drag to entrain particles ahead of the flame and eventually this wind pushes the particles ahead of the flame onto the wall [30], where they do not participate in the explosion. There is evidence of a slight pyrolysis of the outer layer of particles by the quenching flame, but the particles after the explosion are predominantly the original biomass material with the same particle size [Satter, 2012].

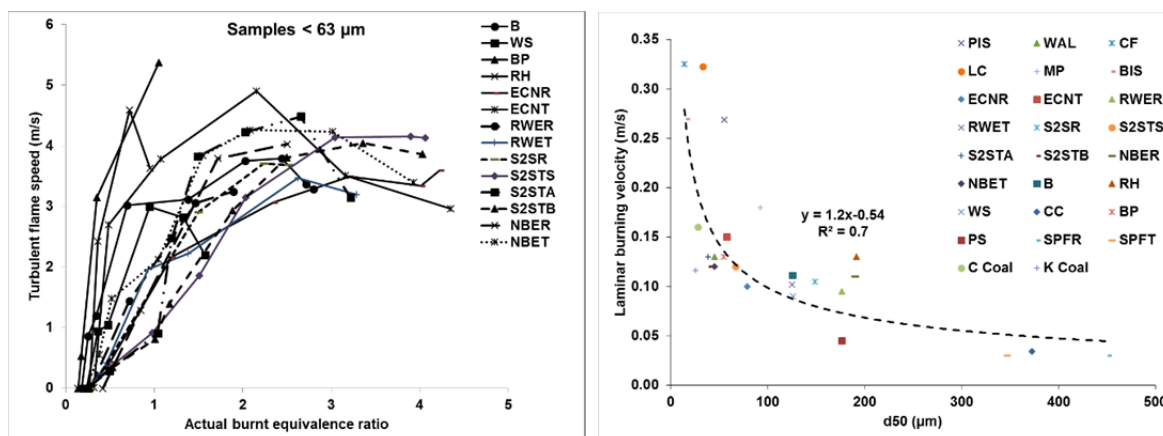


Fig. 1 Turbulent flame speed as a function of  $\phi_{burnt}$

Fig. 2 Peak laminar burning velocity as a function of the particle  $D_{50}$  size

The measured turbulent flame speeds are shown as a function of the burnt equivalence ratio in Fig. 1. For the 28 biomass the peak  $S_T$  varied between 3 and 5.5 m/s. However, the burnt equivalence ratio,  $\phi_{burnt}$ , at which the peak turbulent flame speed occurred was at very rich mixtures, much richer than the peak burning velocity would occur for gases, where the peak reactivity is typically  $\phi=1.05$ . The peak pressure also remained high in the rich mixture region, which is a feature of all dust explosions [Eckhoff, 2003]. The reason for this is that as the flame propagates, the explosion induced wind ahead of the flame will preferentially propagate in the finer particles and aerodynamic drag will result in the larger particles lagging behind the flame front, where they are heated by the hot burnt gases. This generates rich mixtures that are gasified with the release of mainly hydrogen and CO. This volume expansion in rich mixtures keeps the pressure high

There was a significant variation in the peak  $S_T$  for the different biomass and this was related to the differences in particle size. The peak  $S_u$  is shown as a function of  $D_{50}$  in Fig. 2. The range of  $S_u$  is from 0.32 m/s for cornflour to 0.025 m/s for the SPF wood mixture in raw and torrefied form. This  $S_u$  for cornflour is well below the value of 0.65 m/s measured by Dahoe et al. [2002] and 0.55 m/s measured by Satter et al. [2014] using the present equipment, but is similar to the  $S_u$  of 0.25 m/s from the results of Phylaktou et al. [2011]. Commonly available cornflour has a difference in size distribution which gives these differences in  $S_u$ . The most reactive standard biomass was walnut shells with a  $S_u$  of 0.27 m/s. Most of the biomass had  $S_u$  in the range 0.1–0.15 m/s and these are much lower values than for hydrocarbon gases where the maximum  $S_u$  is about 0.4 m/s [Andrews and Bradley, 1972]. The volatile gases evolved from biomass and similar compounds when they are first heated (low temperature pyrolysis) have been determined by TGA FTIR [Basilakis et al., 2001; Hajaligol et al., 2001; Saeed et al., 2015] to be  $CO_2$ ,  $H_2O$ ,  $CO$ ,  $H_2$ ,  $CH_4$ , acetaldehyde, acetic and formic acids, benzene, phenols and a wide range of other minor components. The two inert gases are in the highest concentration and this effectively lowers the CV of the evolved gases. The release of hydrocarbons is very low from biomass and most of the species that are flammable are mixtures of oxygenated species which have a low CV. Fig. 2 shows that quite coarse biomass can still propagate a flame. Coarse particles  $>63\mu m$  and  $<500\mu m$  propagate an explosion [Saeed et al., 2015] in agreement with the trends in Fig. 2.

## 6. Conclusions

A method for determining the  $S_u$  of dusts and pulverised biomass has been developed based on the ISO 1 m<sup>3</sup> dust explosion vessel. Thermocouple arrays were added to determine the turbulent flame speed. Calibration of the turbulence was undertaken using methane-air explosions for the laminar and turbulent case and the turbulence in the ISO explosion vessel was determined as a  $S_T/S_L$  of 4.0–4.7, depending on the dust disperser

used. The derived  $S_L$  was divided by the expansion ratio, based on the measured pressure rise, to determine  $S_u$ . The method gave values of  $S_u$  for HCO dusts (0.32 m/s) and biomass (0.025 – 0.3 m/s) which were lower than for gaseous hydrocarbons. The prime effect on  $S_u$  was the mean particle size,  $D_{50}$ .

### Acknowledgements

The authors acknowledge the financial support to MAS by the Univ. of Eng. and Tech., Lahore, Pakistan. The authors are grateful to the EPSRC Energy Programme (Grant EP/H048839/1) for partial financial support.

### References

- Andrews, G.E. and Bradley, D. 1972. *Combust. Flame*, 18 (3) 133 - 145.
- Andrews, G.E. and Phylaktou, H.N., 2010. In: M. Lackner, F. Winter and A.K. Agarwal (Eds.), *Handbook of Combustion*, Wiley-VCH, Weinheim, p.377.
- Bartknecht, W., *Dust Explosions: Course, prevention, protection*. 1989. Springer London.
- Bartknecht, W., 1993. *Explosionsschutz, Grundlagen und Anwendung*, Springer Verlag, Germany
- Bassilakis, R., Caranglo, R.M., Wojtowicz, M.A. 2001. *Fuel* 80, 1765-1782.
- Cashdollar, K.L. 2000. *J. Loss Prevention in the Process Industries*, 13, 183-199.
- Chippett, S., 1984. *Combust. Flame*, 55, 127-140.
- Dahoe, A. E., Hanjalic, K. and Scarlett, B., 2002. *Powder Technology*, 122, 222-238.
- Eckhoff, R.K. 2003. *Dust Explosions in the Process Industries*, Gulf Professional Publishing, USA.
- European Standard BS EN-1839:2003. Limits of Flammability Measurement Standard for Gases and Vapours.
- European Standard, BS EN 14034-1 2004: Determination of explosion characteristics of dust clouds Part 1: Determination of maximum pressure  $P_{max}$  of dust clouds. British Standards Institute, London.
- European Standard, BS EN14034-2 2006. Determination of explosion characteristics of dust clouds - Part 2: Determination of the maximum rate of explosion pressure rise  $(dP/dt)_{max}$  of dust clouds..
- European Standard BS EN 14994:2007. Gas Explosion Venting Protective Systems.
- European Standard, BS EN 15967:2011. Determination of the maximum explosion pressure and the maximum rate of pressure rise of gases and vapours. British Standards Institute, London.
- European Standard BS EN14491 2012. Dust explosion venting protective systems.
- Gardner, C.L, Phylaktou, H.N. and Andrews, G.E. 2001. Turbulence and Turbulent Burning Velocities in the ISO 1 m<sup>3</sup>, Proc. 17<sup>th</sup> ICDERS, Seattle.
- Hajaligol, M., Waymah, B., Keelor, D. *Fuel* 80 (2001) 1799 – 1807.
- Huescar-Medina, C., Sattar, H., Phylaktou, H.N., Andrews, G.E. and Gibbs, B.M. 2014. Explosion reactivity characterisation of pulverised torrefied spruce wood. Tenth Int. Symp. on Hazards, Prevention, and Mitigation of Industrial Explosions (XISHPMIE) Bergen, Norway.
- Huescar-Medina, C., Andrews, G.E., Phylaktou, H.N. and Gibbs, B.M. 2014 Proc. 10<sup>th</sup> European Conference on Coal Research and its Applications, University of Hull.
- ISO 6184/1. Standard for the Determination of Explosion Indices of Combustible Dusts in Air, 1985.
- Mazarkiewicz and Jorisade. Sixth International Colloquia on Dust Explosions, 1994, 179.
- Meng, A., Zhou, H., Qil, C., Zhai, Y. and Li, Q. 2013. *J. Anal. App. Pyrolysis* 104, 28 – 37.
- National Fire Protection Association (NFPA), 2013, 2017. Guide for Venting of Deflagrations NFPA 68.
- Nagy, J. and Verikas, H.C., 1983. *Development and Control of Dust Explosions*, Marcel Dekker.
- Phylaktou, H.N., Gardner, C.L. and Andrews, G.E., 2011. Flame Speed Measurements in Dust Explosions. Proc. of the Sixth International Seminar on Fire & Explosion Hazards (FEH6), 695-706.. Eds. D. Bradley, G. Makhviladze and V. Molkov. Research Publishing.
- Phylaktou, H.N., Gardner, C.L. and Andrews, G.E., 2011. Flame Speed Measurements in Dust Explosions. Proc. of the Sixth International Seminar on Fire & Explosion Hazards (FEH6), 695-706.. Eds. D. Bradley, G. Makhviladze and V. Molkov. Research Publishing.
- Proust, C. and Veyssiere. B. 1988. *Comb. Sci.Tech.*, 62, 149-172.
- Proust, C., 1993. Experimental Determination of the Maximum Flame Temperature and of the Laminar Burning Velocities for some Combustible Dust/Air Mixtures. Proc. of the Fifth Int. Colloq. on Dust Explosions, Bergen.
- Saeed, M.A., Andrews, G.E., Phylaktou, H.N. Slatter, D., Huéscar-Medina, C. and Gibbs, B.M. 2015. Proc. International Colloquium on the Dynamics of Explosive and Reactive Systems, ICDERS.
- Saeed, M.A., Andrews, G.E., Phylaktou, H.N. and Gibbs, B.M. 2016. Raw and steam exploded pine wood: Possible enhanced reactivity with gasification hydrogen. *Int. Journal of Hydrogen Energy*. In Press.
- Sattar, H., Phylaktou, H.N., Andrews, G.E. and Gibbs, B.M., 2012. Explosions and Flame Prop. in Nut-shell Biomass Powders. Proc. of the IX Int. Sem. on Hazardous Proc. Mats and Ind. Expls (IX ISHPMIE), Krakow.
- Sattar, H., Huescar, C.M., Phylaktou, H.N., Andrews, G.E. and Gibbs, B.M. 2013. Calibration of a 10L Volume Dust Holding Pot for the 1 m<sup>3</sup> Standard Vessel for Use in Low Bulk Density Biomass Explosibility Testing. Proc. Seventh Int. Sem. on Fire and Explosion Hazards (ISFEH7), pp.791-800. Research Publishing.
- Sattar, H., Andrews, G.E., Phylaktou, H.N. and Gibbs, B.M., 2014. *Chem. Eng. Trans.*, 36, 157-162.
- Smoot, L.D. Horton M.D. and Williams, G.A., 1977. *Proc. Comb. Inst.* 16 , 375-387.
- Taylor, S.C. and Smith, D.B. 1995. *Combust. Flame*, 102, 523.
- Wolanski, P. (Ed), 1995. *Dust Explosions*. EC CREDIT Project Contract No. EV5V-CT92-0082.